# Combining cut element methods and hybridization

Erik Burman
University College London

POEMS 2019, CIRM, April 2019

Joint work with:
G. Delay, D. Elfversson, A. Ern, P. Hansbo,
M. Larson, K. Larsson

EPSRC
Engineering and Physical Sciences Research Council

# Outline

1. cutFEM, levelset geometries
2. cutFEM with hybridization, polygonal grains
3. A Hybridized High Order (HHO) method with cut cells

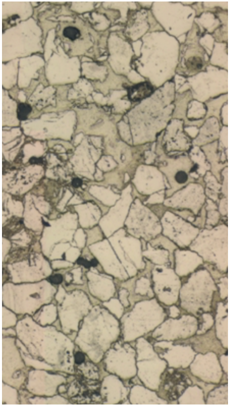

Figure: SEM image of sandstone, width $\approx 1$ mm. [Baud et al. J. of Struct. Geo. 2004].

# Solving PDEs on meshes that are not fitted to the domain

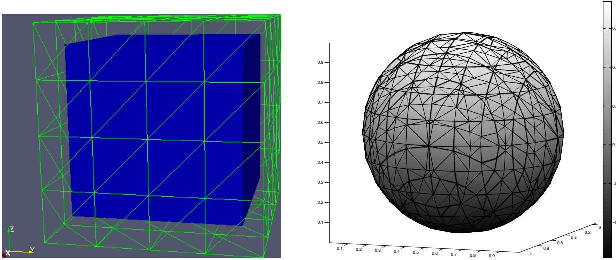

Figure: Can we solve PDEs on embedded domains (left) or embedded surfaces (right)

- **Imposition of boundary conditions**: [Nitsche 1971], [Babuska 1973].
- **Fictitious domain methods:** [Girault, Glowinski 1995], [Angot 1998], [Bertoluzza et al. 2005], [Haslinger, Renard 2009]
- **Unfitted FEM:** [Barrett, Elliott 1987], [Hansbo, Hansbo 2002]
- **Trace finite elements:** [Olshanskii et al. 2009]

# CutFEM - model problem

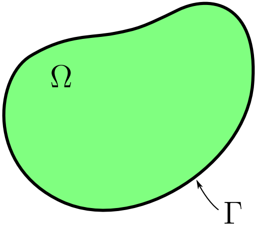


Consider Poisson's equation: $u : \Omega \to \mathbb{R}$ such that

$$\begin{aligned} -\Delta u &= f && \text{in } \Omega \\ u &= g_D && \text{on } \Gamma_D \\ \nu \cdot \nabla u &= g_N && \text{on } \Gamma_N \end{aligned}$$

where $\nu$ is the outward pointing normal of $\Gamma$

# CutFEM

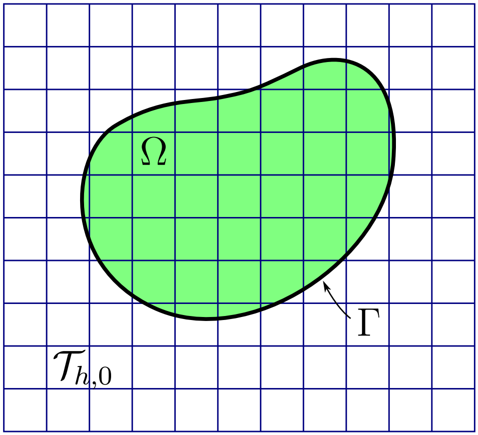

# CutFEM

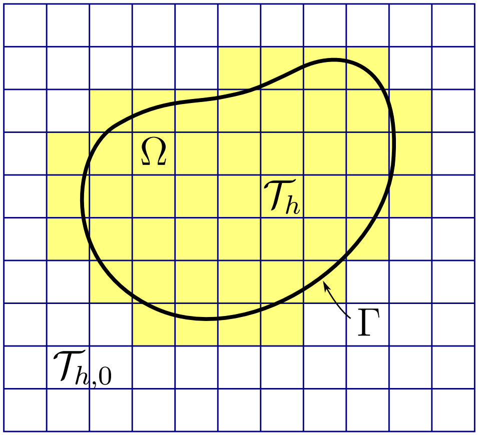

# CutFEM

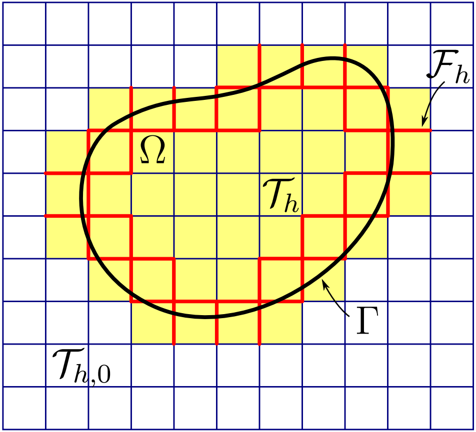

# Mesh and Finite Element Spaces.

Let

- $U_\Omega$ be a polygonal domain such that $\Omega \subset U_\Omega$
- $\mathcal{T}_{h,0}$ be a family of meshes on $U_\Omega$ with mesh parameter $h \in (0, h_0]$
- $\mathcal{T}_h = \{T \in \mathcal{T}_{h,0} : \overline{\Omega} \cap \overline{T} \neq \emptyset\}$
- $\mathcal{T}_\Gamma$ set of elements in $\mathcal{T}_h$, that intersect the boundary $\Gamma$
- $\mathcal{F}_h$ set of interior faces of elements in $\mathcal{T}_\Gamma$
- $V_{U,h} \in H^1(U_\Omega)$ be a finite element space of order $p$ on $\mathcal{T}_{h,0}$ and $V_h = V_{U,h}|_{\mathcal{T}_h}$

Assume that

- $\Gamma$ is smooth (or a polygon with curved boundaries)
- $\Gamma$ "well resolved" by the mesh: any cut cell is divided in two parts, both including a part of the triangle boundary

# CutFEM I

**Method.** Find $u_h \in V_h$ such that

$$A_h(u_h, v_h) = L_h(v_h) \qquad \forall v_h \in V_h$$

where

$$A_h(u_h, v_h) = a_h(u_h, v_h) + s_h(u_h, v_h)$$

- $a_h(u, v)$ and $L_h(v)$: weak forms over $\Omega$, with weak boundary conditions
- Nitsche's method:

$$a_h(u,v) := \int_\Omega \nabla u \cdot \nabla v \, \mathrm{d}x - \int_{\Gamma_D} \Big( \underbrace{\nu \cdot \nabla u v}_{\textit{consistency}} + \underbrace{\nu \cdot \nabla v u}_{\textit{symmetry}} - \underbrace{\frac{\gamma}{h} u v}_{\textit{coercivity}} \Big) \, \mathrm{d}s$$

- Right hand side:

$$L_h(v) = (f, v)_\Omega + (g_N, v)_{\Gamma_N} - (g_D, \nu \cdot \nabla v)_{\Gamma_D} + \beta h^{-1} (g_D, v)_{\Gamma_D}$$

# CutFEM II

- $s_h(u, v)$: stabilization added to make $A_h$ coercive, independently of the cut[1]

$$\|u_h\|^2_{H^1(\mathcal{T}_h)} \lesssim \|u_h\|^2_{H^1(\Omega)} + s_h(u_h, u_h) \lesssim \underbrace{a_h(u_h, u_h)}_{\text{only control of } H^1(\Omega)} + s_h(u_h, u_h)$$

- $s_h$ must also have some weak consistency

$$s(i_h u - u, i_h u - u)^{\frac{1}{2}} \lesssim h^p$$

- Example: penalty on derivative jumps:

$$s_h(u_h, v_h) := \gamma_g \sum_{F \in \mathcal{F}_h} \sum_{l=1}^{p} h^{2l-1} \int_F [D^l_{n_F} u_h][D^l_{n_F} v_h] \, \mathrm{d}s$$

  Here $D^l_{n_F} v$ denotes the $l$th partial derivative in the normal direction, $[x]|_F$ the jump of the quantity $x$ over the face $F$.

- There is now a zoo of different ghost penalty terms, both for cutFEM and TraceFEM. [Lehrenfeld 2018], [Larson et al. 2018]

[1] EB. *Ghost penalty*, C. R. Math. Acad. Sci. Paris 348 (2010), no. 21-22, 1217-1220.

# CutFEM: Main Results (no geometry approximation)

Let the energy norm be defined by

$$|||v|||^2 = \|v\|^2_{H^1(\Omega)} + \|v\|^2_{s_h} + h^{-1}\|v\|^2_{\Gamma_D} + h\|n \cdot \nabla v\|^2_{\Gamma_D}$$

- Coercivity

$$|||v|||^2 \lesssim A_h(v, v) \qquad v \in V_h$$

- Continuity

$$A_h(v, w) \lesssim |||v|||\,|||w||| \qquad v, w \in H^{p+1}(\mathcal{T}_h) + V_h$$

- Interpolation estimate
  - $u^e \in H^{p+1}(\mathcal{T}_h)$ stable extension of $u \in H^{p+1}(\mathcal{T}_h)$ (Stein)
  - $\pi_h : H^{p+1}(\mathcal{T}_h) \to V_h$ optimal interpolation operator

$$|||u^e - \pi_h u^e||| \lesssim h^p \|u\|_{p+1}$$

- A priori error estimates (Modified argument for $H^{1+\epsilon}(\Omega)$, $\epsilon > 0$)

$$\boxed{\|u - u_h\|_{H^1(\Omega)} \lesssim |||u^e - u_h||| \lesssim h^p\|u\|_{p+1}, \qquad \|u - u_h\|_\Omega \lesssim h^{p+1}\|u\|_{p+1}}$$

- Estimate of the stiffness matrix condition number: $\boxed{\kappa(\mathcal{A}) \lesssim h^{-2}}$

# Applications, two-phase flows shape optimization[2] [3] [4]

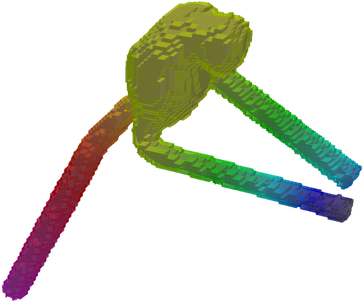

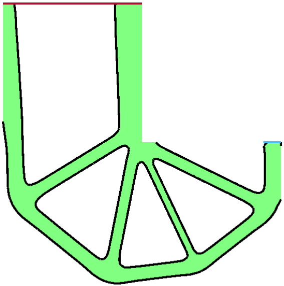

[2]EB, S. Claus, A. Massing, A Stabilized Cut Finite Element Method for the Three Field Stokes Problem, SISC, vol 37 (7), 2015.

[3]S. Claus, P. Kerfriden, A CutFEM method for two-phase flow problems, arXiv:1806.10156

[4]EB, D. Elfverson, P. Hansbo, M. Larson, K. Larsson, *Shape optimization using the cut finite element method*. CMAME (2018).

# Combining cutFEM and hybridization

# cutFEM using hybridization

- Polyhedral boundaries (possibly curved faces)
- Introduce skeleton unknowns
- Motivation
  - Strongly varying diffusion between cells
  - Strongly varying diffusion within a cell
  - Inclusions
  - Coupled PDEs on bulk and surfaces
- Hybridization allows elimination of bulk dofs through static condensation
- The $\Omega_i$ and $\Omega_{0,k}$ discretized on bulk mesh
- No requirement for the meshes to match

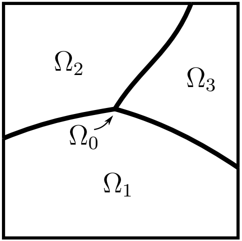


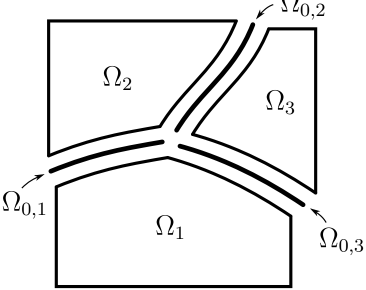

# Bulk and skeleton discretization ($i = 3$, $k = 2$)

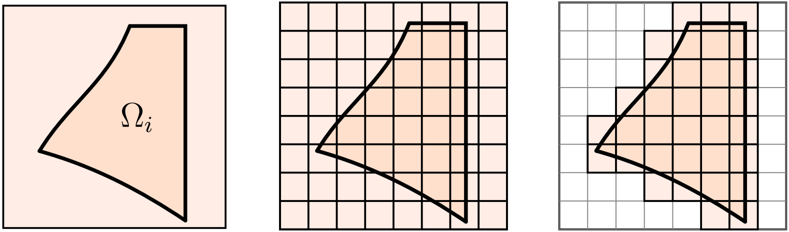


Figure: $U_{\Omega_i}$ $\qquad$ $\mathcal{T}_h(U_{\Omega_i})$ $\qquad$ $\mathcal{T}_{h,\Omega_i} = \mathcal{T}_{h,i}$

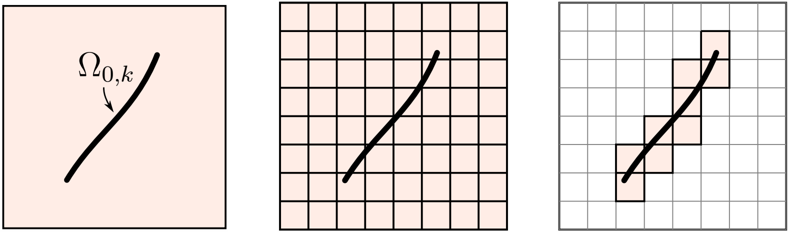


Figure: $U_{\Omega_{0,k}}$ $\qquad$ $\mathcal{T}_h(U_{\Omega_{0,k}})$ $\qquad$ $\mathcal{T}_{h,\Omega_{0,k}} = \mathcal{T}_{h,0,k}$

# Finite element spaces I

- For $O \in \{\Omega_i\}_{i=1}^{N}$ let $V_{h,O}$ be a finite dimensional space consisting of continuous piecewise polynomial functions defined on $\mathcal{T}_{h,O}$
- we also use the simplified notation

$$V_{h,i} = V_{h,\Omega_i}, \qquad \mathcal{T}_{h,i} = \mathcal{T}_{h,\Omega_i} \tag{1}$$

and for $O \in \{\Omega_{0,k}\}_{k=1}^{N_0}$,

$$V_{h,0,k} = V_{h,\Omega_{0,k}}, \qquad \mathcal{T}_{h,0,k} = \mathcal{T}_{h,\Omega_{0,k}}, \qquad \mathcal{T}_{h,0} = \sqcup_{k=1}^{N_0} \mathcal{T}_{h,0,k} \tag{2}$$

- Define the finite element spaces

$$V_{h,0} = \bigoplus_{k=1}^{N_0} V_{h,0,k}, \qquad V_{h,1,N} = \bigoplus_{i=1}^{N} V_{h,i} \tag{3}$$

and

$$W_h = V_{h,0} \oplus V_{h,1,N} \tag{4}$$

# The Poisson interface problem

We consider the following hybridized formulation of the Poisson problem: find $u_0 : \Omega_0 \to \mathbb{R}$ and for $i = 1, \dots, N$, $u_i : \Omega_i \to \mathbb{R}$ such that

$$
\begin{aligned}
-\nabla \cdot a_i \nabla u_i &= f_i && \text{in } \Omega_i && (5)\\
[\![\nu \cdot a \nabla u]\!] &= 0 && \text{on } \Omega_0 && (6)\\
[u]_i &= 0 && \text{on } \partial\Omega_i \cap \Omega_0 && (7)\\
u_i &= 0 && \text{on } \partial\Omega_i \cap \partial\Omega && (8)
\end{aligned}
$$

Here $a_i$, $i = 1, \dots, N$, are positive constants and the jumps operators are defined by

$$
[u]|_{\partial\Omega_i \cap \Omega_0} = u_i - u_0, \qquad [\![\nu \cdot a \nabla u]\!]|_{\partial\Omega_i \cap \partial\Omega_j} = \nu_i \cdot a_i \nabla u_i + \nu_j \cdot a_j \nabla u_j \qquad (9)
$$

where $\nu_i$ is the exterior unit normal to $\Omega_i$.

# The hybridized cutFEM method

- Find $u_h \in W_h$ such that

$$A_h(u_h, v) = l_h(v), \qquad \forall v \in W_h \tag{10}$$

where $W_h$ is defined in (4) and

$$A_h(v, w) = s_{h,0}(v_0, w_0) + \sum_{i=1}^{N} \Big( (a_i \nabla v_i, \nabla w_i)_{\Omega_i} + s_{h,i}(v_i, w_i)$$
$$+ (\beta h_i^{-1} a_i [v]_i, [w]_i)_{\partial\Omega_i} - (\nu_i \cdot a_i \nabla v_i, [w]_i)_{\partial\Omega_i} - ([v]_i, \nu_i \cdot a_i \nabla w_i)_{\partial\Omega_i} \Big)$$
$$l_h(v) = \sum_{i=1}^{N} (f_i, v_i)_{\Omega_i}$$

- To ensure coercivity: stabilization both for the bulk and the skeleton variable.
- In each subdomain discretization equivalent to the fictitious domain case.
- In the fitted case this coincides with the hybridized Nitsche method proposed in [Egger 2009].

# Stabilization forms - bulk and surface ghost penalty

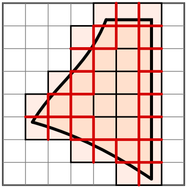

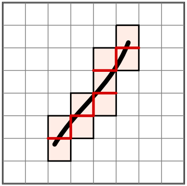

- Define set of faces in the interface zones, $\mathcal{F}_{h,i}$ and $\mathcal{F}_{h,0,k}$
- For each subdomain $\Omega_i$, $1 \leq i \leq N$

$$s_{h,i}(v, w) = \sum_{\ell=1}^{p} c_{d,\ell}\, h^{2\ell-1}([D^{\ell}_{n_F} v], [D^{\ell}_{n_F} w])_{\mathcal{F}_{h,i}} \tag{11}$$

- For each skeleton subdomain $\Omega_{0,k}$, $1 \leq k \leq N_0$ [Larson and Zahedi 2017]

$$s_{h,0,k}(v, w) = \sum_{\ell=1}^{p} c_{d-1,\ell}\, h^{2\ell} \Bigg( \underbrace{(D^{\ell}_{\nu} v, D^{\ell}_{\nu} w)_{\Omega_{0,k}}}_{\text{normal stabilization}} + \underbrace{([D^{\ell}_{n_F} v], [D^{\ell}_{n_F} w])_{\mathcal{F}_{h,0,k}}}_{\text{jump stabilization}} \Bigg) \tag{12}$$

# Main results, error estimates

- energy norm (norm thanks to a Poincaré inequality):

$$|||v|||_h^2 = \|v_0\|_{s_{h,0}}^2 + \sum_{i=1}^{N} \|\nabla v_i\|_{\Omega_i,a_i}^2 + h\|\nabla v_i\|_{\partial\Omega_i,a_i}^2 + h^{-1}\|[v]_i\|_{\partial\Omega_i,a_i}^2 + \|v_i\|_{s_{h,i}}^2$$

- The following error estimates hold:

$$\boxed{|||u - u_h|||_h^2 \lesssim h^{2p}\|u_0\|_{H^{p+1/2}(\Omega_0)}^2 + \sum_{i=1}^{N} h^{2p}\|u_i\|_{H^{p+1}(\Omega_i)}^2}$$

- Also $L^2$-norm error estimates.
- Analysis: fictitious domain argument in each subdomain + Poincaré
- Let $\hat{S}$ denote the stiffness matrix associated with the Schur complement, then

$$\boxed{\text{condition number: } \kappa(\widehat{S}) \lesssim h^{-1}\left(\min_{1\le i\le N} d_{\Omega_i}\right)^{-1}} \tag{13}$$

where $h$ is the (uniform) mesh size and $d_{\Omega_i}$ is the diameter of domain $\Omega_i$.

## Computional experiments
## cutFEM and hybridization

# Example 1: Three Subdomains. I

- Three subdomains
- $a_i = i,\ i = 1, 2, 3.$
- *Global Background Grid.*
  All meshes are extracted from the same background grid of $Q_2$ elements
- *Single Element Interfaces.*
  The mesh on each subdomain is constructed independently, some as quadrilateral meshes and some as triangular, and we equip all subdomain meshes with $Q_2/P_2$ elements. On each skeleton subdomain we use a single $Q_4$ element.

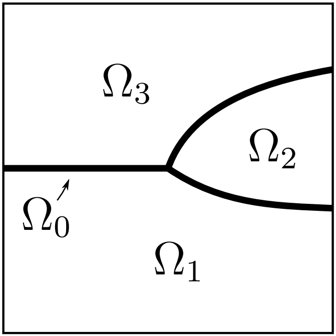

# Example 1: Three Subdomains. II

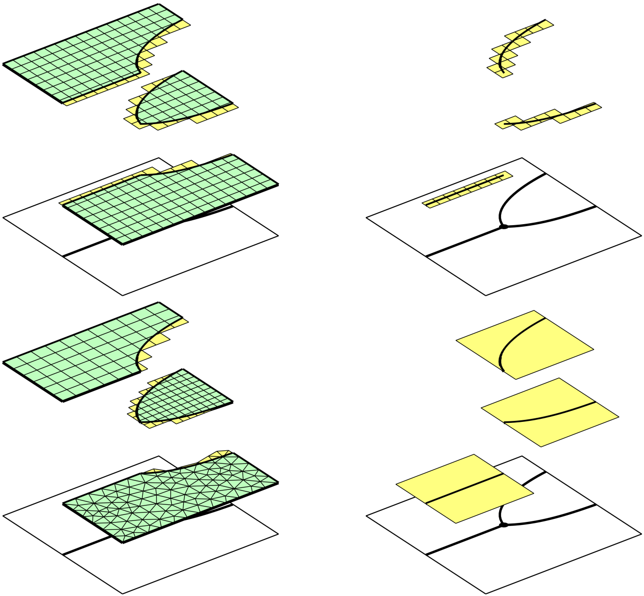

# Example 1: Three Subdomains. III

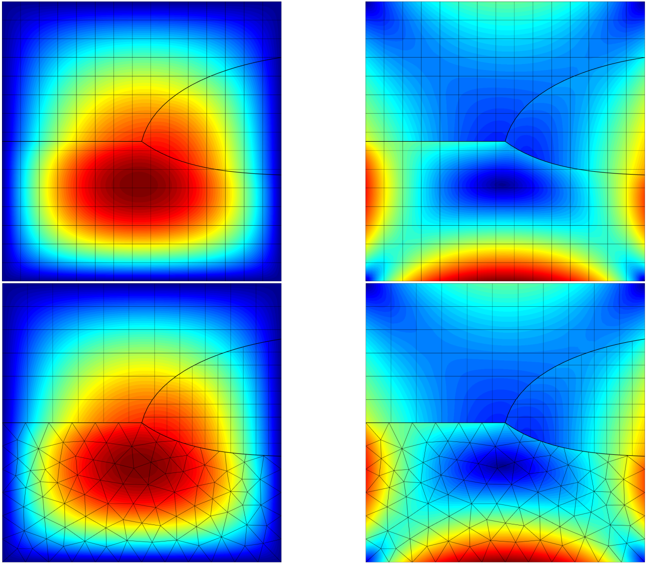

# Example 2: Convergence study. I

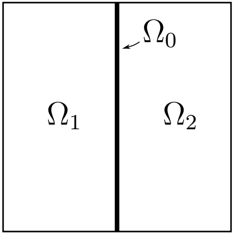


Figure: Domain

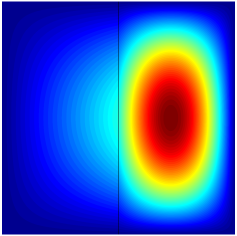

Solution

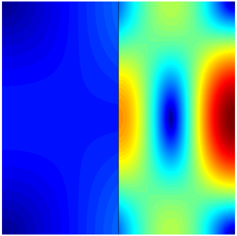

Gradient magnitude

Problem with known exact solution used in convergence studies.

- The domain is the unit square $[0, 1]^2$ partitioned into two subdomains
- material coefficients $a_1 = 1$ and $a_2 = 2\pi - 1$.

# Example 2: Convergence study. II

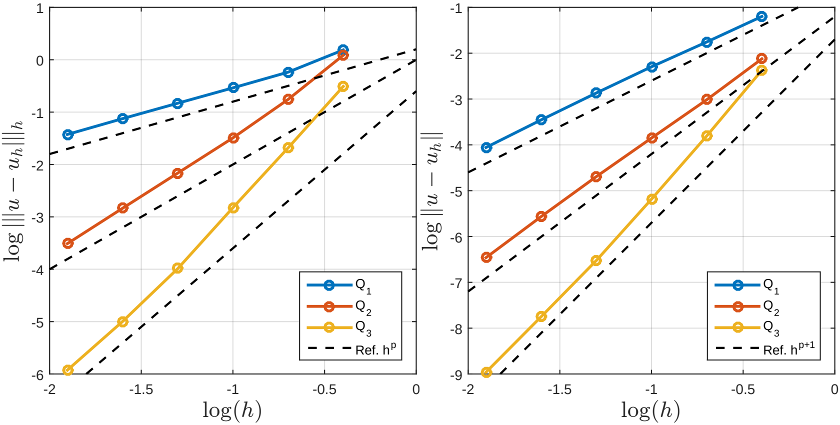


Figure: Convergence studies using meshes all from the same background grid. In all meshes the same elements are used ($Q_1$–$Q_3$). Left: energy norm. Right: $L^2$-norm.

# Example 2: Convergence study. III

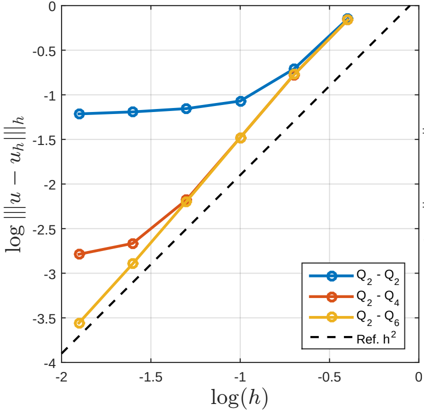


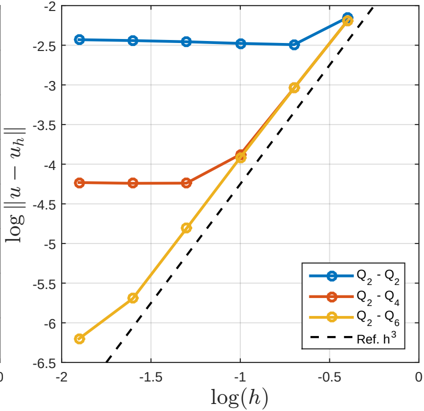


Figure: Convergence studies using non-matching meshes for the subdomains and a single polynomial for each skeleton subdomain. On the subdomains $Q_2$ elements are used and on the skeleton subdomains $Q_2$–$Q_6$ polynomials are used. Left: energy norm. Right: $L^2$-norm.

# Example 3: Voronoi Diagram. I

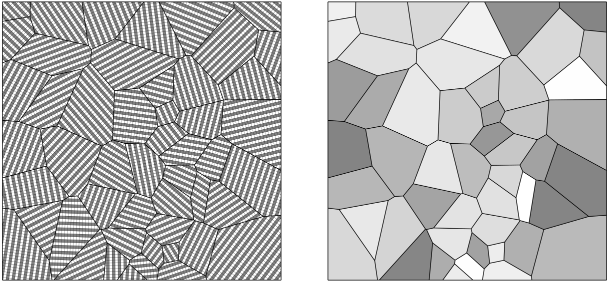

Figure: Subdivisions of the unit square $[0, 1]^2$ generated from Voronoi diagrams featuring varying material coefficients. Left: Domain with a randomly oriented mesh in each subdomain and a material coefficient $a$ which alternates between 1 and 1000 row-wise in the mesh. Right: Domain with material coefficient $a \in [0.01, 1]$ which is constant within each subdomain and chosen using a uniformly distributed random variable.

# Example 3: Voronoi Diagram. II

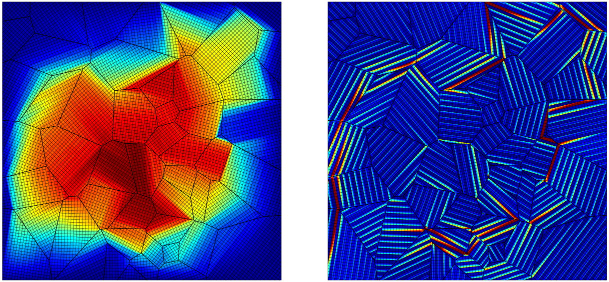

Figure: Numerical solution $u_h$ and gradient magnitude $|\nabla u_h|$ on a Voronoi diagram subdivision with a fine scale material coefficient pattern. On each subdomain a mesh fitted the row-wise alternating material coefficient is set-up. The numerical solution is approximated using $Q_2$ elements in the bulk. On each skeleton subdomain is approximated by a single $Q_4$ element.

# Example 3: Voronoi Diagram. III

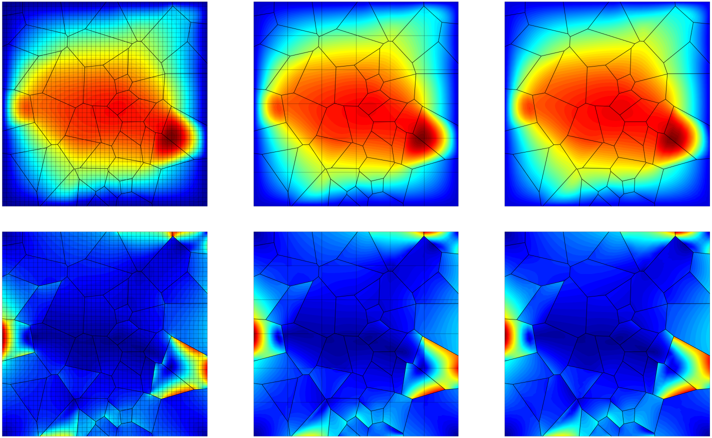

Figure: Numerical solution $u_h$ and gradient magnitude $|\nabla u_h|$ on a Voronoi diagram subdivision with subdomain-wise constant material coefficient. Left: $Q_2$ elements on meshes generated from one fine grid. Middle: $Q_2$ elements on meshes generated from one coarse grid with a mesh size in the same order as the subdomain sizes. Right: A single $Q_2$ element on each subdomain and skeleton subdomain.

## Hybrid High Order method and cut cells

# Hybrid High-Order methods on unfitted meshes

- Introduced in [Di Pietro, Ern 15]
- $k$ polynomial degree

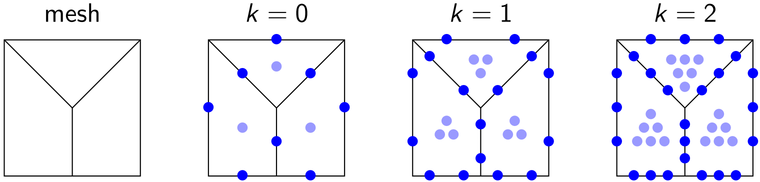


- in the case of **unfitted meshes**, we consider $k$ on the faces and $\mathbf{k+1}$ on the cells

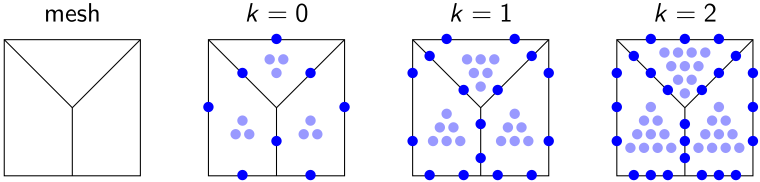


- The discrete problem is assembled cell-wise

# Interest of unfitted meshes

- Enables the use of simpler meshes to mesh intricate geometries
- Fitted HHO is not adapted to treat curvilinear boundaries
- Moving interfaces and boundaries handled without mesh modification
- A first work on elliptic interface problems [B., Ern 18]
- Keypoint: robustness with respect to bad cuts by **agglomeration of cells** [Johansson, Larson 13] (using polyhedral meshes)
- Other works on discontinuous Galerkin with unfitted interfaces [Bastian, Engwer 09], [Massjung 12], [Gürkan, Massing 18] also related [Cangiani, Georgoulis, Sabawi 2018]
- Hybridized dG and unfitted interfaces [Cockburn, Qiu, Solano 14], [Gürkan et al. 16]

## Model problem and its HHO discretization

# Model problem

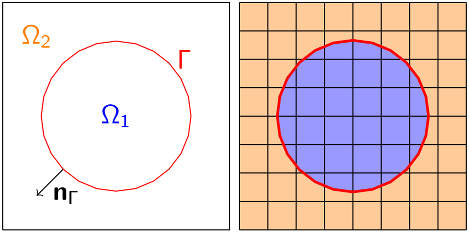


- domain $\Omega \subset \mathbb{R}^d$
- interface $\Gamma$
- subdomains $\Omega_1$, $\Omega_2 \subset \Omega$
- define the jump:
  $[\![y]\!]_\Gamma = y_{|\Omega_1} - y_{|\Omega_2}$

$$
\begin{aligned}
\kappa_1 \Delta u &= f \text{ in } \Omega_1 \\
\kappa_2 \Delta u &= f \text{ in } \Omega_2 \\
[\![u]\!]_\Gamma &= g_D \text{ on } \Gamma, \\
[\![\kappa \nabla u]\!]_\Gamma \cdot \mathbf{n}_\Gamma &= g_N \text{ on } \Gamma, \\
u &= 0 \text{ on } \partial\Omega,
\end{aligned}
$$

# The local discretization: uncut cells (1/3)

- Let $T$ a cell of $\mathcal{T}_h$

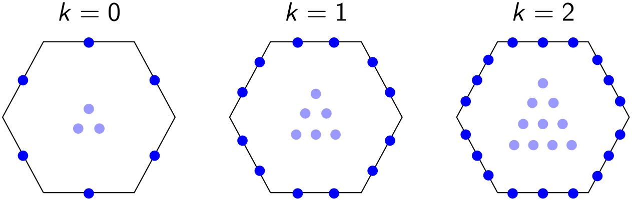


- $\mathbf{n}_T$ outward normal to $T$
- The local unknowns are $u_T \in \mathbb{P}^{k+1}(T)$ on the cell $T$ and the polynomials $u_F \in \mathbb{P}^k(F)$ on every face $F$ composing the boundary of $T$
- $\hat{u}_T = (u_T, u_{\partial T})$ with $u_{\partial T} = (u_F)_{F \in \mathcal{F}_T}$

# The local discretization: uncut cells (2/3)

Two important elements:

- A gradient reconstruction operator $\mathbf{G}_T^k(\hat{u}_T) \in \mathbb{P}^k(T;\mathbb{R}^d)$ such that for every $\mathbf{q} \in \mathbb{P}^k(T;\mathbb{R}^d)$,

$$(\mathbf{G}_T^k(\hat{u}_T), \mathbf{q})_T = -(u_T, \mathrm{div}\, \mathbf{q})_T + (u_{\partial T}, \mathbf{q} \cdot \mathbf{n}_T)_{\partial T}$$

- A stabilization operator

$$s_T(\hat{u}_T, \hat{v}_T) = h_T^{-1} \sum_{F \in \mathcal{F}_T} (\Pi_F^k(u_F - u_T), v_F - v_T)_F$$

(if cell unknowns in $\mathbb{P}^{k+1}(T)$)

Goal: to enforce matching of cells and faces unknowns

# The local discretization: uncut cells (3/3)

- The local operator

$$a_T(\hat{u}_T, \hat{v}_T) = \kappa(\mathbf{G}_T^k(\hat{u}_T), \mathbf{G}_T^k(\hat{v}_T))_T + \kappa s_T(\hat{u}_T, \hat{v}_T)$$

- The local right–hand side

$$\ell_T(\hat{v}_T) = (f, v_T)_T$$

# The local discretization: cut cells (1/4)

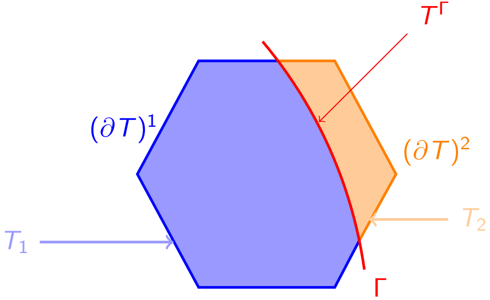


- Decomposition of the cut cells

$$\overline{T} = \overline{T_1} \cup \overline{T_2}$$

- Decomposition of the cut faces

$$\partial(T_1) = (\partial T)^1 \cup T^\Gamma \qquad \partial(T_2) = (\partial T)^2 \cup T^\Gamma$$

# The local discretization: cut cells (2/4)

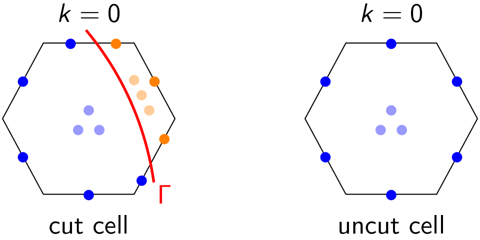


- We **double** the unknowns on cut cells/faces in the spirit of [Hansbo, Hansbo 02] for cut FEM
- $u_{T_1} \in \mathbb{P}^{k+1}(T_1)$, $u_{T_2} \in \mathbb{P}^{k+1}(T_2)$
- $u_{(\partial T)^1} \in \mathbb{P}^{k}((\partial T)^1)$, $u_{(\partial T)^2} \in \mathbb{P}^{k}((\partial T)^2)$
- $\hat{u}_T = (u_{T_1}, u_{(\partial T)^1}, u_{T_2}, u_{(\partial T)^2})$
- No dof on $T^\Gamma$

# The local discretization: cut cells (3/4)

- For $i = 1, 2$, a gradient reconstruction operator $\mathbf{G}^k_{T_i}(\hat{u}_T) \in \mathbb{P}^k(T_i; \mathbb{R}^d)$ such that for every $\mathbf{q} \in \mathbb{P}^k(T_i; \mathbb{R}^d)$,

$$(\mathbf{G}^k_{T_i}(\hat{u}_T), \mathbf{q})_{T_i} = -(u_{T_i}, \mathrm{div}\, \mathbf{q})_{T_i} + (u_{(\partial T)^i}, \mathbf{q} \cdot \mathbf{n}_T)_{(\partial T)^i} + (u_{\overline{T_i}}, \mathbf{q} \cdot \mathbf{n}_T)_{T^\Gamma}$$

  Can also use Nitsche's method on the interface [B., Ern 18]

- Lehrenfeld-Schöberl stabilization operator

$$s_T(\hat{u}_T, \hat{v}_T) = h_T^{-1} \sum_{i \in \{1,2\}} \kappa_i \sum_{F_i \in \mathcal{F}_{T_i}} (\Pi^k_{F_i}(u_{F_i} - u_{T_i}), v_{F_i} - v_{T_i})_{F_i}$$

# The local discretization: cut cells (4/4)

- Assumption : $\kappa_1 \geq \kappa_2$
- The local operator

$$a_T(\hat{u}_T, \hat{v}_T) = \sum_{i \in \{1,2\}} \kappa_i (\mathbf{G}^k_{T_i}(\hat{u}_T), \mathbf{G}^k_{T_i}(\hat{v}_T))_{T_i} + (\kappa_2 \nabla u_{T_2} \cdot \mathbf{n}_\Gamma, [\![ v_T ]\!]_\Gamma)_{T^\Gamma}$$
$$+ \eta \kappa_2 h_T^{-1} ([\![ u_T ]\!]_\Gamma, [\![ v_T ]\!]_\Gamma)_{T^\Gamma} + \kappa_2 ([\![ u_T ]\!]_\Gamma, \nabla v_{T_2} \cdot \mathbf{n}_\Gamma)_{T^\Gamma}$$
$$+ s_T(\hat{u}_T, \hat{v}_T)$$

- The local right–hand side

$$\ell_T(\hat{v}_T) = \sum_{i \in \{1,2\}} (f, v_{T_i})_{T_i} + (g_N, v_{T_2})_{T^\Gamma}$$
$$+ \eta \kappa_2 h_T^{-1} (g_D, [\![ v_T ]\!]_\Gamma)_{T^\Gamma} + \kappa_2 (g_D, \nabla v_{T_2} \cdot \mathbf{n}_\Gamma)_{T^\Gamma}$$

- **Several variants** are possible by modifying the reconstruction.

# The global discretized problem

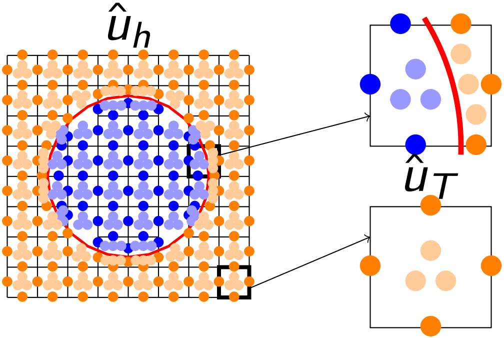


- $\hat{u}_h = \{\hat{u}_T\}_{T\in\mathcal{T}_h}$: the global set of dofs.
- The problem is assembled cell–wise
- find $\hat{u}_h$ such that

$$a_h(\hat{u}_h, \hat{v}_h) = \ell_h(\hat{v}_h) \text{ for every } \hat{v}_h$$

- with $a_h(\hat{u}_h, \hat{v}_h) = \sum_{T\in\mathcal{T}_h} a_T(\hat{u}_T, \hat{v}_T)$ and $\ell_h(\hat{v}_h) = \sum_{T\in\mathcal{T}_h} \ell_T(\hat{v}_T)$

# Numerical analysis, unfitted HHO method

# Stability

- Two assumptions :
  - interface well resolved
  - no bad cuts of volume cells thanks to agglomeration

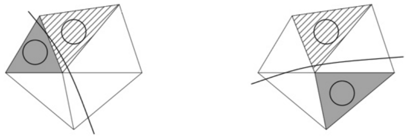

- Energy norm (local/cut cells):

$$\|\hat{v}_h\|_*^2 := \sum_{i=1}^{2} \left( \kappa_i \|\nabla v_{T_i}\|_{T_i}^2 + \kappa_i h_T^{-1} \|\Pi_{(\partial T)^i}^k (v_{T_i} - v_{(\partial T)^i})\|_{(\partial T)^i}^2 \right) + \kappa_2 \eta h_T^{-1} \|[\![ v_T ]\!]_\Gamma\|_{T^\Gamma}^2$$

## Lemma

"Cut-robust" trace inequality implies coercivity, i.e. for $\eta$ large enough, for every $\hat{v}_h$, we have $\|\hat{v}_h\|_*^2 \lesssim a_h(\hat{v}_h, \hat{v}_h)$

# Approximation

- Consider $E_i : \Omega_i \to \mathbb{R}^d$ stable extension operator
- If the mesh is fine enough, for every $T$, there exists $T^\dagger \subset \mathbb{R}^d$, with $T \in T^\dagger$ such that the $L^2$-projections, $\Pi^{k+1}_{T^\dagger} E_1(u))_{|T_1}$, and $\Pi^{k+1}_{T^\dagger} E_2(u)_{|T_2}$ is an optimal approximation [Burman, Ern 18]
- In the analysis, face approximation $\Pi^k_{(\partial T)^1} u$ and $\Pi^k_{(\partial T)^2} u$, handled through orthogonality/stability
- define $\hat{I}^k_T(u) = ((\Pi^{k+1}_{T^\dagger} E_1(u))_{|T_1}, \Pi^k_{(\partial T)^1} u, (\Pi^{k+1}_{T^\dagger} E_2(u))_{|T_2}, \Pi^k_{(\partial T)^2} u)$

## Lemma

For every $v \in H^{k+2}(\Omega)$, we have

$$\|\mathbf{G}^k_{T_i}(\hat{I}^k_T(v)) - \nabla v\|_{T_i} \lesssim h^{k+1} |E_i(v)|_{H^{k+2}(T^\dagger)}$$

# Consistency

- Consider the discrete error $\hat{e}_h = \hat{I}_h^k(u) - \hat{u}_h$, with $\hat{I}_h^k(u)$ defined through the local approximation operator $\hat{I}_T^k(u)$.

## Lemma

For $\hat{e}_h = \hat{I}_h^k(u) - \hat{u}_h$, we define

$$\mathcal{F}(\hat{v}_h) = a_h(\hat{e}_h, \hat{v}_h)$$

and we have

$$\boxed{|\mathcal{F}(\hat{v}_h)| \lesssim \left( \sum_{T \in \mathcal{T}_h} \|\nabla u - \mathbf{G}_T^k(\hat{I}_T^k(u))\|_T^2 + \ldots \right)^{1/2} \|\hat{v}_h\|_*}$$

# Error estimate

## Theorem

We have

$$\|u - \hat{u}_h\|_* \leq \|u - \hat{I}_h^k(u)\|_* + \Big( \sum_{T \in \mathcal{T}_h} \|\nabla u - \mathbf{G}_T^k(\hat{I}_h^k(u))\|_T^2 + \dots \Big)^{1/2}$$

Then when $u \in H^{k+2}(\Omega)$, we have

$$\boxed{\|u - \hat{u}_h\|_* \lesssim h^{k+1} \|u\|_{H^{k+2}(\Omega)}}$$

- $\| \cdot \|_*$ energy norm
- proof :

$$\|\hat{e}_h\|_*^2 \lesssim a_h(\hat{e}_h, \hat{e}_h)$$
$$\lesssim \Big( \sum_{T \in \mathcal{T}_h} \|\nabla u - \mathbf{G}_T^k(\hat{I}_T^k(u))\|_T^2 + \dots \Big)^{1/2} \|\hat{e}_h\|_*$$

and triangular inequality

## Computational experiments
## HHO with cut cells

# Geometry

- Developments in the DiSk++ library (available on github)
- $\Omega = (0,1)^2$
- $\Gamma$ circle, radius $R = 0.33$
- Homogeneous cartesian mesh

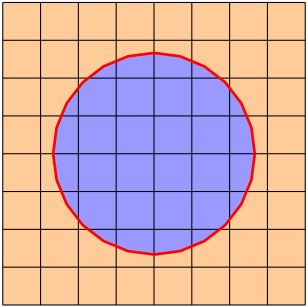

# A contrast problem

- From [Burman, Guzmán, Sánchez, Sarkis 16]
- $\kappa_1 = 1$, $\kappa_2 = 10^4$, $g_D = g_N = 0$
- Exact solution

$$u(\mathbf{x}) = \frac{r^2}{\kappa_1} \text{ in } \Omega_1$$

$$u(\mathbf{x}) = \frac{r^2}{\kappa_2} + R^2\left(\frac{1}{\kappa_1} - \frac{1}{\kappa_2}\right) \text{ in } \Omega_2$$

- $r^2 = (x_1 - 0.5)^2 + (x_2 - 0.5)^2$

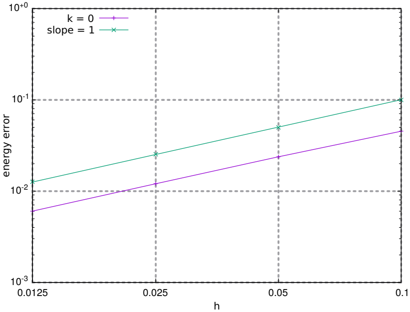


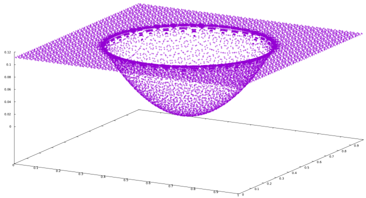

# A problem with a jump in the solution

- From [Huynh, Nguyen, Peraire, Khoo 13]
- Exact solution

$$u(\mathbf{x}) = \sin(\pi x_1)\sin(\pi x_2) \text{ in } \Omega_1$$
$$u(\mathbf{x}) = e^{x_1}\cos(x_2) \text{ in } \Omega_2$$

- $\kappa_1 = \kappa_2 = 1$

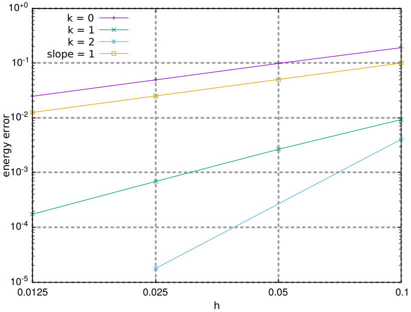


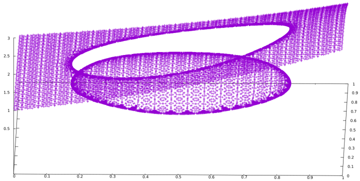

# Concluding remarks

- Hybridized cutFEM
  - an unfitted hybridized method for polytopal geometries
  - requires stabilization in the interface zone
  - mesh resolve local cell small scale features + static condensation
  - a flexible tool for the coupling of pdes on the bulk and on surfaces (see figure).
- HHO method with cut elements
  - allows for (relatively) straightforward discretization of curved boundaries
  - interface coupling - cell model
  - requires cell agglomeration for stability
  - extension to Stokes' problem under way

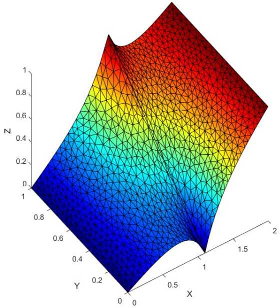

# Main results, error estimates

- energy norm:

$$|||v|||_h^2 = \|v_0\|_{s_{h,0}}^2 + \sum_{i=1}^{N} \|\nabla v_i\|_{\Omega_i,a_i}^2 + h\|\nabla v_i\|_{\partial\Omega_i,a_i}^2 + h^{-1}\|[v]_i\|_{\partial\Omega_i,a_i}^2 + \|v_i\|_{s_{h,i}}^2$$

- $|||\cdot|||_h$ is a norm thanks to a Poincaré inequality
- The following error estimates hold (assuming regularity)

$$\boxed{|||u - u_h|||_h^2 \lesssim h^{2p}\|u_0\|_{H^{p+1/2}(\Omega_0)}^2 + \sum_{i=1}^{N} h^{2p}\|u_i\|_{H^{p+1}(\Omega_i)}^2}$$

and, with $s \in [1,2]$ depending on the regularity of the dual problem,

$$\boxed{\sum_{i=1}^{N} \|u_i - u_{h,i}\|_{\Omega_i}^2 \lesssim h^{2p+2(s-1)}\|u_0\|_{H^{p+1/2}(\Omega_0)}^2 + \sum_{i=1}^{N} h^{2p+2(s-1)}\|u_i\|_{H^{p+1}(\Omega_i)}^2}$$

- Analysis: fictitious domain argument in each subdomain + Poincaré

# Main results, the Schur complement I

- Define the operator $T_h : V_{h,0} \to V_{h,1,N} = \bigoplus_{i=1}^N V_{h,i}$ such that

$$A_h(v_0 + T_h v_0, 0 \oplus w) = 0, \qquad \forall w \in V_{h,1,N} \tag{14}$$

where the notation $0 \oplus w$ indicates that the component in $V_{h,0}$ is zero.

- Define the Schur complement form on $V_{h,0}$ by

$$S_h(v_0, w_0) = A_h(v_0 + T_h v_0, w_0 + T_h w_0), \qquad v_0, w_0 \in V_{h,0} \tag{15}$$

- Solution using the Schur complement:
we have the $A_h$-orthogonal splitting $W_h = (I + T_h)V_{h,0} \perp (\{0\} \oplus V_{h,1,N})$. Thus $u_h = (I + T_h)u_{h,0} + (0 \oplus u_{h,1,N})$ where $u_{h,0} \in V_{h,0}$ is the solution to

$$S_h(u_{h,0}, w_0) = l_h((I + T_h)w_0), \qquad \forall w_0 \in V_{h,0} \tag{16}$$

and $u_{h,1,N}$ is the solution to

$$A_h(0 \oplus u_{h,1,N}, 0 \oplus w) = l_h(w), \qquad \forall w \in V_{h,1,N} \tag{17}$$

We note that (17) decouples and can be solved subdomain wise.

# Main results, the Schur complement II

- Let $\{\varphi_i\}_{i=1}^D$ be the basis in $V_{h,0}$ and denote the expansion by

$$v = \sum_{i=1}^{D} \widehat{v}_i \varphi_i \tag{18}$$

- The stiffness matrix associated with the Schur complement is defined by

$$(\widehat{S}\widehat{v}, \widehat{w})_{\mathbb{R}^D} = S_h(v, w) \tag{19}$$

## Theorem (Condition Number Estimate)

*The condition number $\kappa(\widehat{S})$ satisfies the estimate*

$$\boxed{\kappa(\widehat{S}) \lesssim h^{-1}\left(\min_{1\leq i\leq N} d_{\Omega_i}\right)^{-1}} \tag{20}$$

*where $h$ is the (uniform) mesh size and $d_{\Omega_i}$ is the diameter of domain $\Omega_i$.*

# Local Schur complement

- Close to the Hybrid Discontinuous Galerkin (HDG) method
  - Polyhedral method
  - Primal point of view
- The dof attached to the cells can be **eliminated** by a **local Schur complement**

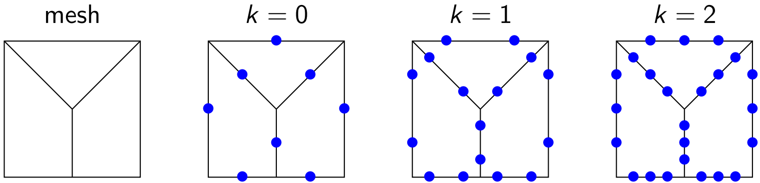


- The global problem to solve comprises only the dof attached to the faces
- We recover the polynomials of the cells using post–processing